TECHNICAL PAPER

CrossMark

Experimental investigations on the incremental sheet forming of commercial steel ASTM A653 CS-A G90 to predict maximum bending effort

Pablo D. Valle[1] · Fred Lacerda Amorim[2] · Dalberto D. Da Costa[1] · Paulo V. P. Marcondes[1]

Abstract

Single point incremental sheet forming stands out mainly by using traditional CNC machines to produce small batches of parts or customized products. Thus, any excessive force in the process may compromise the integrity of the machining center or even damage the component itself, limiting its formability. Hence, this work presents the design of experiments to investigate the behavior of mechanical forming forces and optimize the process. The main goal was to build a mathematical function by regression analysis that best represents the theoretical model. The equation proposed here allows to locate and estimate the maximum effort F_{z_peak} based on five input parameters: tool diameter; wall angle; sheet thickness; vertical step size; and tool feed rate. At the same time, determine the set of data that maximize the required formability. The test was carried out using a carbide coated tool K40 and a commercial sheet steel ASTM A653 CS-A G90. The following were found: the feed rate is not significant and can be maximized to reduce production time; the tool diameter and wall angle are significant, and they have a slight influence on the forces and both depends on the design area; the vertical step size is significant and the most important parameter to leveling the process to reach maximum formability. Finally, the sheet thickness is obviously significant; however, it is also specified by the design.

Keywords Incremental sheet forming · Regression analysis · Maximum effort · Formability · Vertical step size

1 Introduction

Incremental sheet forming (ISF) was presented for the first time by Matsubara in Japan, in the late 1990s and was designed aiming to reduce necessary equipment and to increase production flexibility [1–3]. Currently, the development of ISF is aligned with the fourth industrial revolution, which means that the technology is focused in modernizing conventional processes to make feasible new procedures of sheet metal forming and reduce production time, material waste, energy consumption, and to integrate

several equipment simultaneously [4]. Single point incremental forming (SPIF) is a relatively new process used to manufacture deep drawn components. The basic idea is to locally print the part with a hemispherical tool that follows a complex path as shown in Fig. 1a.

The advantage of ISF is its great flexibility, because only one tool is required in free bulging. It is also possible to use a die in order to increase the quality of the final geometry. The applied forces are not very high, so the die can be manufactured with low-cost materials. The major disadvantage of this process is that the forming time is very long. Therefore, SPIF is more appropriate for small-scale production, for creating prototypes and for producing internal or external shapes (Fig. 1b) and profiles in a sheet metal using a shaped tool controlled by CAM on CNC machines. Some of the outstanding features, such as flexibility, low-cost tooling, and quick response to the market, make it suitable for various applications, for example, it is capable to produce various irregular complex components and highly customized medical parts [5].
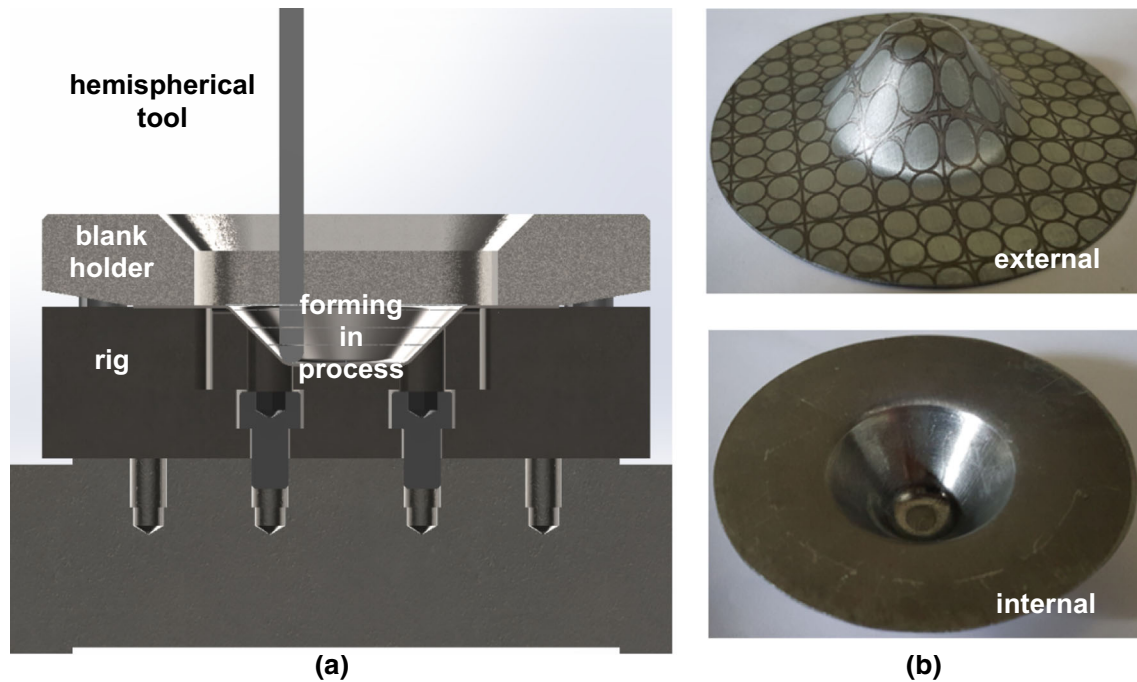
✉ Pablo D. Valle
  pablo.valle@ufpr.br

1   Department of Mechanical Engineering, Federal University of Paraná, Jardim das Américas, Curitiba CEP:81531-980, Brazil

2   Polytechnic School, Pontifícia Universidade Católica do Parana, Curitiba, Brazil

🖄 Springer

Fig. 1 SPIF technology: **a** forming in process, and **b** workpiece formed

High strains can be achieved with the incremental forming; in fact, forming limit diagrams (FLD) for the SPIF shows strains up to 300% of a classical stamping process [6]. Additionally, prediction of maximum effort in ISF provides understanding of the deformation mechanics, parts failure and a means of real-time control and, consequently, its optimization.

The efficient prediction of the forming force is one of the main limitations for the further development, although some authors attempted to bridge the existing gap by finite element method. Even though finite element (FE) models are commonly used to predict forming force for various forming processes, it is significantly time-consuming for the ISF process. This is partly because the sheet deformation during the process is localized and it continuously changes over the whole process [7].

Aiming for quick estimations of the maximum effort, some researchers have proposed analytical models [8]. They found a regression formula that allows to compute the components of forming force, F_x, F_y, and F_z with a good precision (largest error around 6%). Additionally, F_z has been the most critical component for the ISF process. So that, they divide F_z into two forces, one defined such as F_{z_steady}, component in steady state, usually when the process is running stable and only planar deformation occurs, it means the material is been basically stretching by the tool.

A second force is called F_{z_peak}, maximum effort component, usually when the tool is bending the sheet metal in

the beginning of the process and, above all, where the highest force in the process is normally reached. So that, F_{z_peak} becomes the main force to be investigated as it is limited by the technological characteristics of the part being formed.

Meanwhile, it was also found different stress and strain states for different material flow at 20° and 60° of wall angle. Now, depending on the material flow and properties it becomes hardener to forming; consequently, higher deformation forces will be needed [9].

In this field, preliminary experimental investigations were carried out by Jeswiet et al. [10] who measured the force trend in SPIF by using a cantilever type of sensors, mounted on the tool. They investigated tangential force F_t, axial force F_a, and radial force F_r. The forces measured were for 1.21-mm-thick material, AA 3003-0, being formed from flat sheet into a truncated pyramid shape. It can be seen that the maximum effort encountered was around $F_a = 450$ N in the axial z-direction. The most important finding was that the forming force is higher on the beginning of pushing down, i.e., the axial force F_a is higher than the resultant of F_t and F_r. Being so, F_a or F_{z_peak} must be the main force to be monitored on the SPIF [11, 12].

In terms of sustainability, the single point incremental forming requires more machine energy to perform all process than a regular forming. However, it is clear that incremental forming provides higher customization and less burr to the piece; consequently, this combination could

save material usage. The balance between energy consumption by the machine and the material production itself is the center point nowadays. Therefore, it is very important to minimize forces in the incremental sheet forming to enlarge its application and contribute on global energy saving [13].

Traditional stamping process usually requires higher efforts to bending, drawing, and stretching the material part than incremental sheet forming. Nevertheless, the most ISF critical stage in terms of force appears in the beginning of the process and, most of all, it does not have any relationship with the piece geometry or size. So that, parameters like incremental step, tool diameter, and wall angle must be combined and optimized to reduce forces and make the ISF process as efficient as possible [14, 15].

In terms of ISF formability, it becomes clear that when applied temperature to the process, by the tool rotation, the part deformation is higher than the one reached on environmental temperature. It also tends to reduce the maximum required effort to locally forming the piece. This phenomenon occurs by the slipping of between the tool and the material surface. So that, the piece surface could be damaged or even the material properties could be changed [16].

ISF was applied to stainless steel AISI 304, and it was found that for a constant incremental step size both, feed and tool rotation, influence the formability and thinning limit of the component. A maximum reduction in sheet thickness of around 50% was observed [17].

Taking into account the effects of deformation modes from bending, drawing, and stretching to predict effort, an efficient analytical model was proposed on the SPIF process of aluminum metal sheets 7075-O. The main force trend was attributed to the bending effect of the sheet in the early phase of the process, called first stage. The second stage of the process is the combined effects of sheet thinning and strain hardening, when the metal is basically stretched by the tool in planar condition. Hence, the axial force in z-direction in the beginning of the forming process became very important to determine the feasibility of SPIF in terms of quality part and machine integrity. So that, this maximum effort in the beginning is called: F_{zp} or F_{z_peak}—the peak value of the measured force in z-direction at the entrance of the tool. Additionally, it was registered that a general empirical model able to predict forming force for other material and process design needs to be investigated under a different range of process conditions and material [18].

Thus, there is a gap in terms of technical information on the single point incremental sheet forming of commercial steel ASTM A653 CS-A G90 and, above all, to propose a consistent equation to predict the maximum effort in z-

direction, F_{z_peak}. This force F_{z_peak} must be estimated by a robust design of experiments.

So that, in particular, this paper will focus on the validation and accuracy of the efficient force prediction model of a commercial sheet steel ASTM A653 CS-A G90 by a statistical technique design of experiments (DoE).

2 Experimental procedure

The current work is mainly focused on the maximum forming force evaluation F_{z_peak} under the influence of some process parameters: tool diameter, wall angle, sheet thickness, step size and feed rate. A series of tests were performed following the DoE statistical strategy, full factorial 2^5 with confidence interval set at 99% which reflects a significance level of 0.01. The equipment selected for conducting the research on the SPIF was a CNC machining center with hemispherical coated carbide tools and a dedicated acquisition data system (Fig. 2a). A special rig to clamp the workpiece (WP) was also developed (Fig. 2b).

On the machine table was a steel rig in which the specimen could be clamped in such a way that no material may flow into the forming area as shown in Fig. 2b. Between this fixture and the milling machine work-surface, a table-type force sensor was mounted too. This was a piezoelectric dynamometer Kistler multicomponent type 9129AA and connected to it was a complementary Kistler 5070A charge amplifier to measure three-component forces, F_x, F_y, and F_z. With these apparatuses, the force exerted upon the part by the tool was recorded on a computer based data acquisition system at 120 Hz for each channel. The workpiece was assembled into a fixture with a clamping plate fixed by screws, 12Nm each.

Tests have been performed with hemispherical K40 carbide tools with diameters of $d_t = 5$ mm, $d_t = 6$ mm and $d_t = 8$ mm. Although no additional lubricant was applied in the present work, all the tools were coated with aluminum titanium carbo-nitride (AlTiCN) by a PVD coating process to reduce friction coefficient and, so that, increase the ISF formability.

The experiments were carried out at the wall angle of 40°, 50°, and 60° (Fig. 3a), to ensure safety and avoid any damage to the workpiece. Besides that, each complete test was made up of seven contours generated transverse to the long axis of the cone (Fig. 3b). The tool first plunges down into the sheet metal one-step size 3, called vertical step size; then, it moves along the contour traveling clockwise the entire path at this level. After that, the tool moves back to the entrance position and it must move deeper to follow the next contour. The proportion of these steps is governed by both the desired vertical step size Δz from one contour to the next and by the steepness of the wall angle α. In this

Fig. 2 Experimental apparatus: **a** CNC machine with data acquisition, and **b** special rig

(a)   (b)
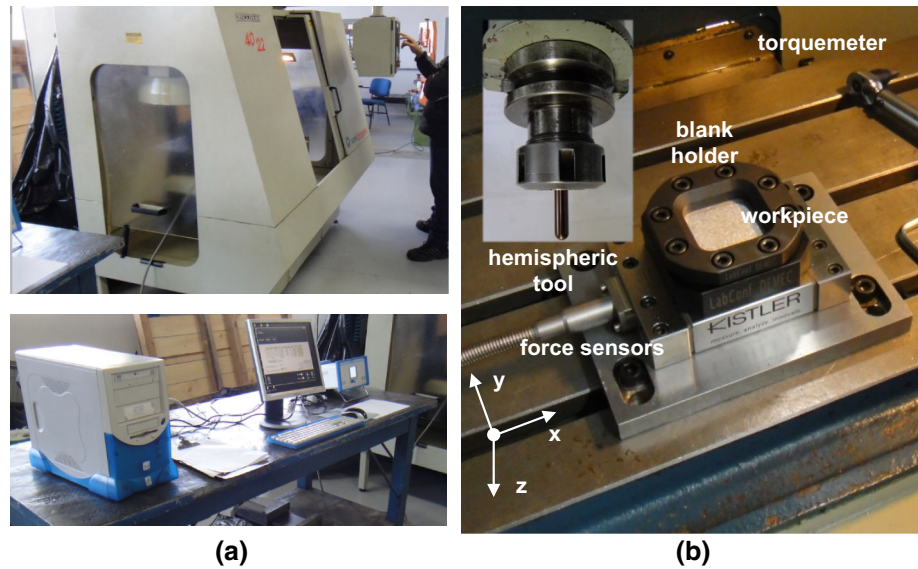
Fig. 3 Truncated cone generated: **a** wall angle, and **b** step size height ($h_{max} = 7X \Delta z$)

(a)

(b)
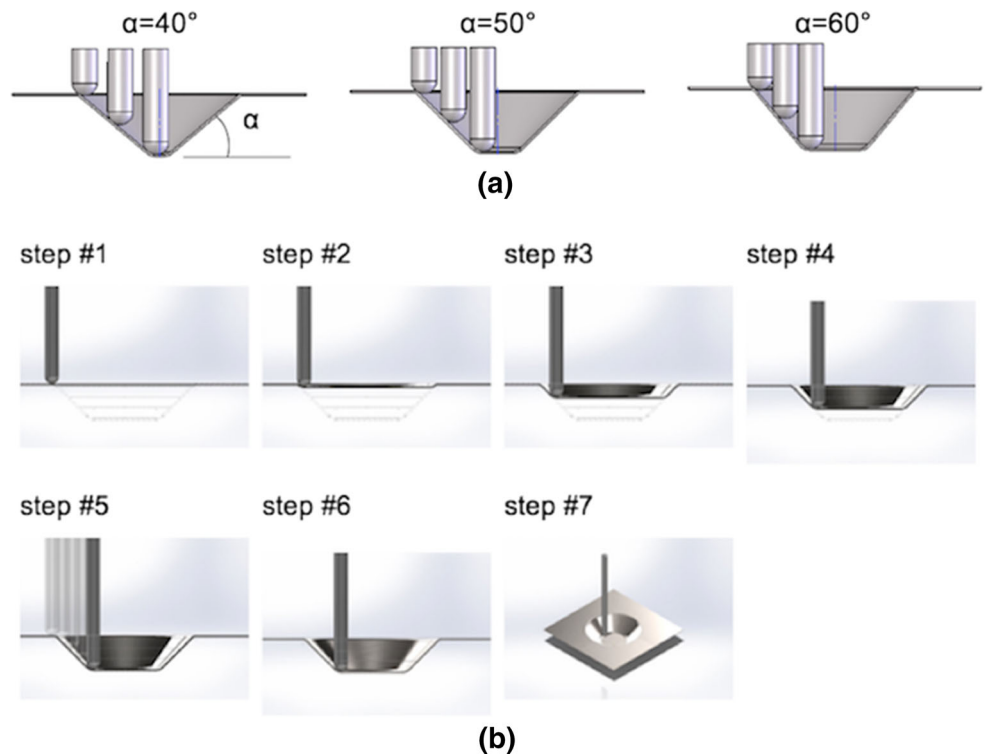
work, the following vertical step sizes were chosen: $\Delta z = 0.4$ mm, $\Delta z = 0.6$ mm, and $\Delta z = 0.8$ mm. In this investigation, free tool rotation speed was chosen so that the tool rolls on the plate at the mean radius of the contact area. The feed rate was 150, 175, and 200 mm/min.

The material used in this research to investigate the prediction force was a commercial steel sheets ASTM A653 CS-A G90 zinc coated commonly used for manufacturing several automotive components, architectural paneling, and in civil construction. The chemical compositions, as shown in Table 1, were specified by the material supplier. Ultimate strength is between 230 and 250 MPa with a yield strength of 215 MPa. Total elongation during tensile test when using 50 mm initial gauge length is around 45%. It was chosen 0.43, 0.65, and 0.80 mm thick for the experiments.

The tool path strategy was defined so that the truncated cones were formed in a stepwise manner with many contours. All the cones were designed with the same major diameter of 40 mm but with a smaller cone height for a

Table 1 Chemical composition

Material	Mass (%)			
	C	P	S	Mn
ASTM A653 CS-A G90	0.100 max	0.030 max	0.035 max	0.600 max

smaller inclination of the wall due to the geometric constraint. The forming forces for each contour were recorded continuously during this process for three orthogonal components (F_x, F_y, and F_z). Thereby, according to the DoE method and being $k = 5$, the number of observations is 32 (a complete 2^5 factorial design).

In this experimental design, three replicates were performed to estimate the variance (experimental error) caused by slightly different experimental conditions. Note that true replication provides an estimate of the error or noise in the process and allows for more precise estimates of effects. These designs were useful for fitting first-order models (which detect linear effects). Additionally, to provide information on the existence of curvature 10 center points were included in the experimental plan.
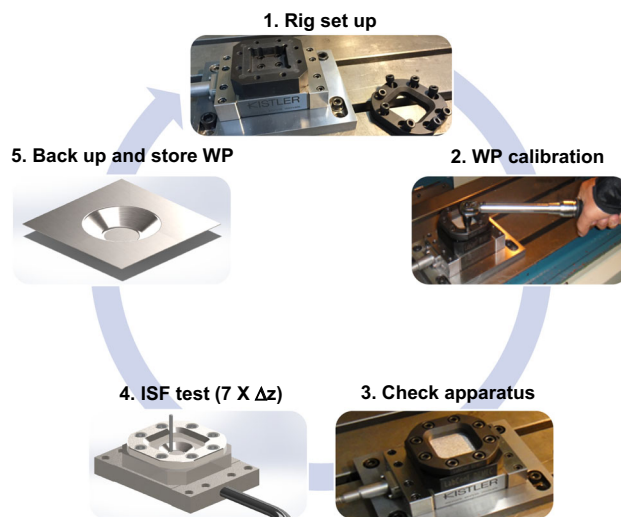
Thereby, 106 tests were carried out to predict forming force in this complete full factorial DoE. Despite the methodological recommendation to randomize the standard order of the tests where possible, in this work the sequence was organized to enable the execution of all tests within a reasonable period of time and, overall, to reduce the chances of errors during the experiment due to the adjustment complexity of all devices involved. Minitab V17 was applied for statistical analysis. According to the previous approach, the five main factors are summarized in Table 2, establishing the sequence from "A" to "E."

In order to assure a robust and standardized systematic for all activities during the cycle tests, all the actions were well defined from start to finish for each experimental workpiece performed. The sequence of all steps in each workpiece (WP) tested can be seen in Fig. 4.

For the part geometry and tool path, forces were measured in three directions corresponding to a cartesian
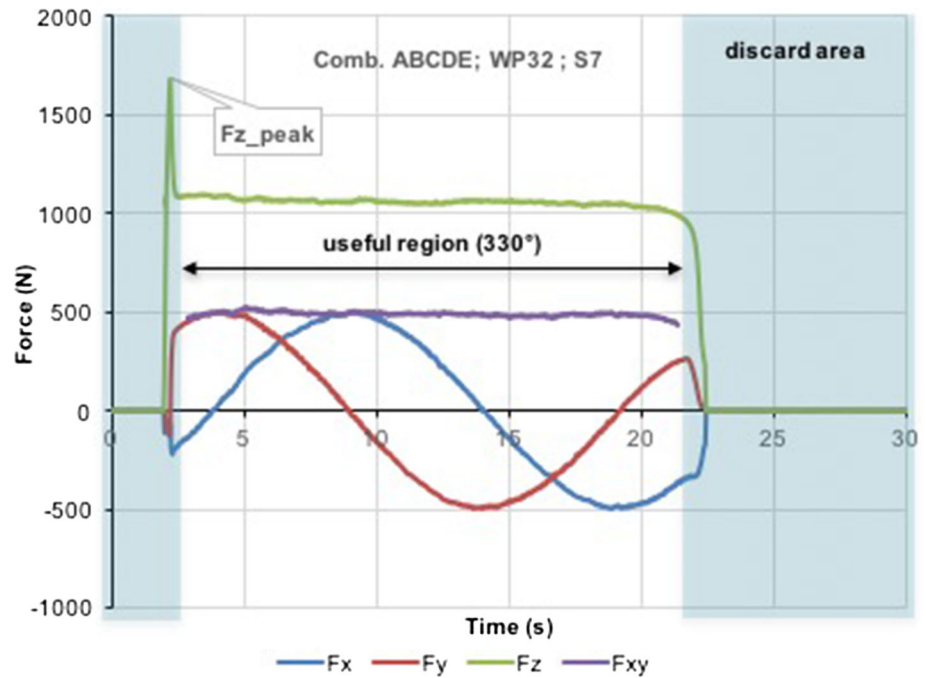

Fig. 4 Sequence of each complete workpiece tested

coordinate system. These three force components F_x, F_y, and F_z were then combined into a total force vector F_R see Eq. (1). The force F_z was the maximum forming force applied in the vertical direction. F_x and F_y were the in-plane forces exerted on the sheet metal.

$$F_R = F_x + F_y + F_z \qquad (1)$$

Figure 5 shows the standard behavior of all forces monitored on each workpiece tested. This graphic refers to the seventh step size (S7) and to the ABCDE combination of experimental planning, which means test number 32 (WP32). The contour equivalent to 330° was defined as a useful region for the steady-state treatment of force prediction, i.e., the initial and final 15° of the deformation process was discarded. However, the highest deformation load in z-direction, called F_{z_peak}, always occurred at the first 15°. This force F_{z_peak} becomes the most important force in SPIF because it reaches the process limits first, then comes steady-state forces F_x, F_y, and F_{z_steady}.

Figure 6 shows F_z vertical force evolution behavior along the seven vertical steps size of the ISF process (S1 to S7) for the WP32. It remains clear that the F_{z_peak} force is continuously increasing and it has the greater magnitude for all steps in all experimental planning. It is mainly due to the drawing process in z-direction just in the beginning of the ISF. However, there is a stabilization of the F_z force after the initial impact of the tool, called steady state (F_{z_steady}).

Table 2 High (+ 1), low (− 1), and standard (0) settings for a full factorial 2^5 DoE

Factors	Levels		
	− 1	0	+ 1
A. Diameter d_t (mm)	5	6	8
B. Wall angle α (°)	40	50	60
C. Thickness t (mm)	0.43	0.65	0.80
D. Step size Δz (mm)	0.40	0.60	0.80
E. Feed f (mm/min)	150	175	200

Fig. 5 F_x, F_y, F_z, and F_{z_peak} versus time. Combination ABCDE, WP 32, step 7

Fig. 6 F_z and F_{z_peak} versus time. Combination ABCDE, WP 32, steps 1–7
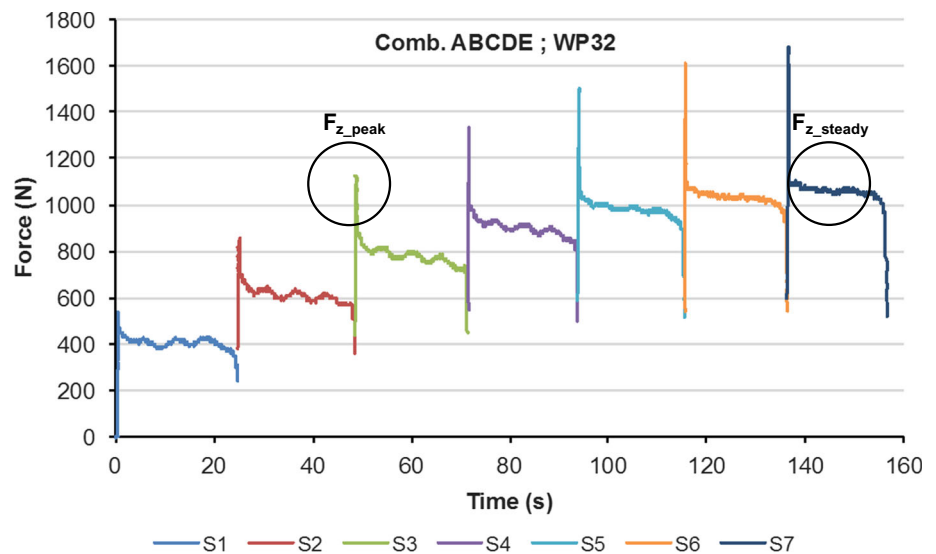

After the fifth step size, F_{z_steady} tends to stabilize due to the thinning of the sheet metal; consequently, the planar load necessary for the stretching process in xy-direction increases little. On the other hand, in the first two steps size, the statistical analysis can be discarded since these two points concentrate significant perturbation but do not compromise the part quality nor the integrity of the CNC machine.

Thus, in order to verify the statistical behavior of the main ISF process forces, F_R and F_{z_peak}, the linear regression curves of the most critical points observed in the experiment are plotted. These points refer to the combination number 32 of DoE 2^5, i.e., the test ABCDE in which

all ISF process parameters are set to the highest level. There are also three replications in this case, WP32 (workpiece 32), WP64 (workpiece 64), and WP96 (workpiece 96). The regression analysis of the model in a simple way considering only F_R and F_{z_peak} forces versus the vertical increment Δz from step three to seven can be observed in Fig. 7. The coefficients of determination R^2 for each equation are very good and similar, $R^2 > 0.96$. Being so, the fit quality of the model that tends to better explain the phenomenon is equivalent in both regressions. Besides that, the maximum bending effort F_{z_peak} remains critical for all steps, and consequently, the main parameter to be controlled to assure part integrity and process optimization.

Fig. 7 Linear regression: F_{z_peak} and F_R. Comb. ABCDE, means WP32, WP64, and WP96
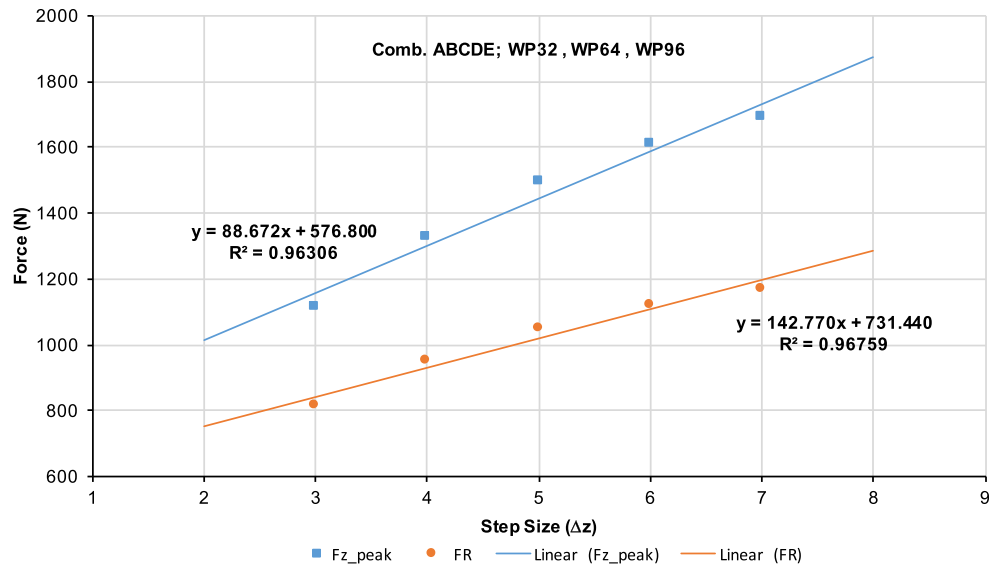
Therefore, the quality of the response is acceptable and could be considered in the upcoming DoE linear regression to simplify the statistical analysis. It also remains clear that the bending effort in z-direction F_{z_peak} is the most critical in terms of formability and machine integrity, since it is the greatest load acting in the SPIF process as shown in Fig. 7.

3 Results and discussion

It was decided to use the F_{z_peak} force as the dependent variable of the experiment under analysis for the proper DoE force prediction. This force tends to set the boundaries of the SPIF process in terms of loading limits. Figure 8

presents the normal plot of the standardized effects for the DoE and the significant factors.

Additionally, all significant effects are shown in Table 3.

Figure 9 shows a picture of the fitted means for the three levels tested (-1, 0, $+1$) of each main factor. It is inferred that the central point for all the main effects is centered; that is, a linear behavior could be considered for all the independent variables in this experimental design.

Therefore, the following deductions can be recorded from the fitted means for the F_{z_peak} force and the five main effects will be discussed in the next items.
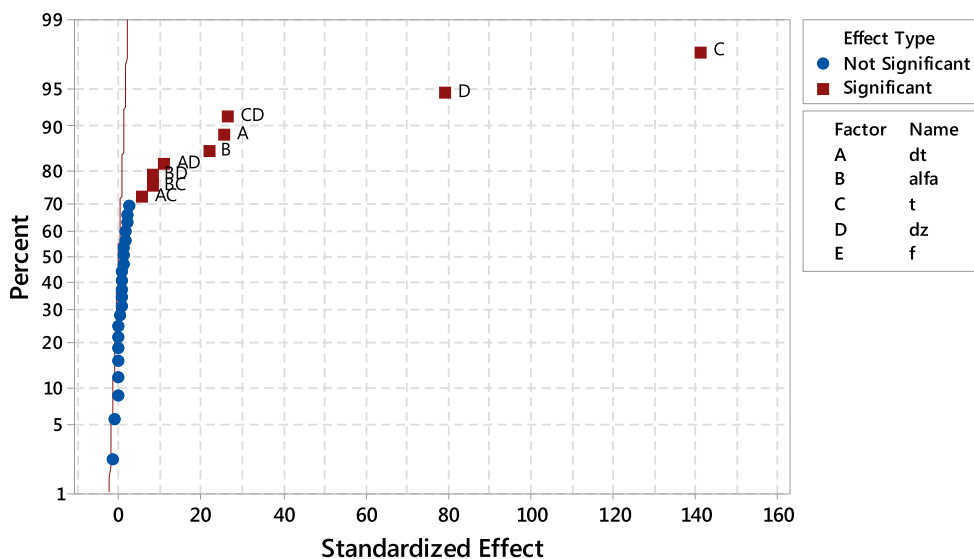
Fig. 8 Normal plot of the standardized effects. F_{z_peak} at step seven, $\alpha = 0.01$

Table 3 List of significant effects

Relevancy order	Factor	Effect
1	C	t
2	D	Δz
3	CD	$t * \Delta z$
4	A	d_t
5	B	α
6	AD	$d_t * \Delta z$
7	BD	$\alpha * \Delta z$
8	BC	$\alpha * t$
9	AC	$d_t * t$

3.1 d_t and α effects

There is a very similar picture of the behavior of the main effects for the tool diameter d_t and for the wall angle α. Both main factors are significant, and a linear regression model behavior can be considered.

The increase in the main factor does not represent a large increase in the magnitude of the maximum force F_{z_peak}. The final geometry of the part to be formed directly impacts the diameter of the tool and the wall angle. Thus, the smaller the radius present in the design of the part the smaller will be the diameter of the tool needed for the respective forming of the desired shape. On the other hand, the greater the angle present in the design of the part the greater will be the forming load required. Consequently, the tool diameter and the wall angle are influenced by the shape specifications resulting from the design of the product, limiting the possible dimensions of its adjustment.

However, in terms of tool stiffness, the larger the minor radius required on the part, the better and the more robust the tool becomes. Ambrogio et al. [19] said that the more extensive the contact area between the tool and the part more lubricant between forming tool (punch) and specimen is needed to prevent excessive friction and get better formability.

Additionally, a critical phenomenon that must be monitored is the ratio of the tool length and its diameter, because vibrations can arise in the case of great relationships, possibly weakening the tool itself, as well as impregnating damages to the stamped sheet.

In terms of the wall angle, Petek et al. [15] investigated its influence on the incremental forming of sheet metal DC05, 1 mm thick, and proposed that the maximal attainable wall angle by the cone-shaped part prior to the crack occurrence is 70°. Meanwhile, Jeswiet et al. [10] found that the maximum values of force occur at a wall angle of 60°. This peak value indicates the sheet is approaching the maximum force value that it can sustain, similar to the ultimate tensile strength observed in engineering stress–strain diagrams.

3.2 t and Δz effects

The main factors, sheet thickness t and step size Δz, present a similar photograph, and both are considered significant to the process with strong influence on the value of the dependent variable F_{z_peak}. In terms of sheet thickness, there is a greater variation between the load obtained for the low level (-1) and the load obtained for the high level ($+1$), points 480 and 1180 N, respectively.

On the other hand, in terms of increment Δz, the variation between levels is somewhere around 400 N, points 630 N and 1030 N. This shows a tendency for a greater increase in the F_{z_peak} forming force as the thickness t increases than the growth observed as the increment Δz increases. Of course, this consideration must be carefully taken into account at this moment, since the thickness of the sheet is basically a design parameter, while increment Δz is a process parameter.

So that, Δz tends to be the most important process parameter when adjusting the process. The F_{z_peak} forming
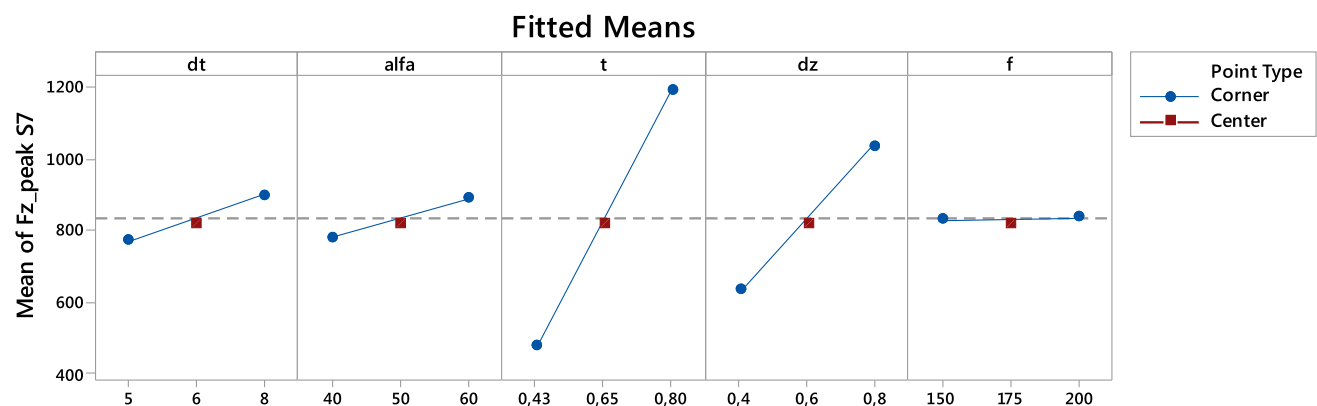
Fig. 9 Main effects plot for F_{z_peak} at step seven, $\alpha = 0.01$

force for $t = 0.43$ mm and all other main factors positioned at the high level (+ 1) are similar to the F_{z_peak} forming force where $t = 0.80$ mm and all other factors are positioned at the low level (− 1).

Thus, the process parameters can be clearly manipulated to minimize the loads even though they have to form thick sheets. Additionally, reducing the increment Δz tends to increase the total depth of forming process. It means to achieve higher formability. Between this and that, it is possible to combine the main factors properly and then to minimize the loads acting on the part, reaching very large forming depths.

3.3 *f* effect

The DoE statistical evaluation of the tool feed f indicates that the respective main factor is not significant. However, in terms of process parameter, the greater the tool feed f, the shorter the production time of the part. It can be concluded that the main factor f can be adjusted to the highest possible value for the process under development without causing a significant increase in the maximum forming force F_{z_peak}, and consequently, it is possible to reduce the production time of the sheet. Always observing sensitive aspects in relation to the integrity of the system such as vibration of the tool or even damage to the surface to be formed due to slipping. According to Tiburi [20], the lubrication between the parts in contact significantly increases the formability of the sheet and, in parallel, reduces the risk of adhesion between the respective tool and workpiece materials.

3.4 *t* and Δz interaction

The interaction of the effects t and Δz is significant, and it is noticed that the growth of the forming efforts is not proportional for the two factors; that is, the function that represents the model Δz is less sensitive than the one that represents the parameter t. As previously discussed, the factors can be considered regression models with linear adjustment, as well as the effect of the interaction. On the other hand, the specification of the sheet thickness and the material itself are from the design area. Therefore, the viability of the use of the CNC machining center in the incremental sheet forming by minimizing the efforts should be done primarily through the Δz factor. In this scenario, it is also assumed that the clamping sheet system is feasible within the machine table limits and, above all, suitable for the required clamping pressure. That is, there is only the parameter Δz that can be adjusted to minimize the deformation loads. The growth of F_{z_peak} due to the impact on increasing Δz is less than the impact due to the increasing the thickness t, which means that, by increasing the sheet

thickness t, Δz cannot be decreased in the same proportion under risk of exceeding the resistance limits of the machining, rig, or part.

3.5 d_t and Δz, α and Δz, α and t, d_t and t interactions

The interactions of the factors d_t and Δz, α and Δz, α and t, and d_t and t, are all significant with linear behavior. The variation in the F_{z_peak} force is much more sensitive with respect to the Δz factor than the one observed with respect to the tool diameter d_t. Thus, there is a favorable aspect regarding to apply bigger tool diameter for forming parts, since the reduction in the tool diameter does not imply in significant decrease in the force F_{z_peak}. Moreover, the tool diameter reduction can weaken the tool itself and, eventually, lead to its rupture.

The behavior of the wall angle α is similar to the tool diameter d_t in relation to the vertical step size Δz; that is, larger angles can be formed without significant increase in the force F_{z_peak}. It should be noted that the wall angle is also a design feature. Having in mind that this option may limit the forming depth a compromise must be taken into account on a case-by-case basis.

The behaviors of the interactions α and t, and, d_t and t are similar, so, at this point, the product wall angle α, tool diameter d_t, and, in particular, sheet thickness t, are factors influenced by the design specifications, as discussed previously. Thus, the margin for manipulating the parameters becomes narrow, since this situation cannot be easily changed. However, both the wall angle α and the tool diameter d_t have a slight influence on the increase in the force F_{z_peak}.

Therefore, the thickness t is the parameter of greatest influence on the forming loads and, as such factor is due to the product design area, it becomes, in addition, a sine qua non condition to minimize the efforts produced through the other process variables, especially optimizing step size Δz.

The tests that presented possible problems—outliers—were left out of the experiment. Considering for the DoE analysis only the tests with stable behavior. After this, the graphs of Fig. 10 were produced for the respective residual analysis.

The Shapiro–Wilk test was used to evaluate the normality of the residues. The value found for p value was 0.031, accepting the hypothesis of residual normality, since the significance level is 0.010. Simple descriptive statistics were applied to confirm that the mean of the residues is zero in addition to normal behavior. Once the residue normality is accepted, it was possible to analyze the homoscedasticity of the estimators of the multiple linear regression model, concluding that the behavior is non-biased and consistent.
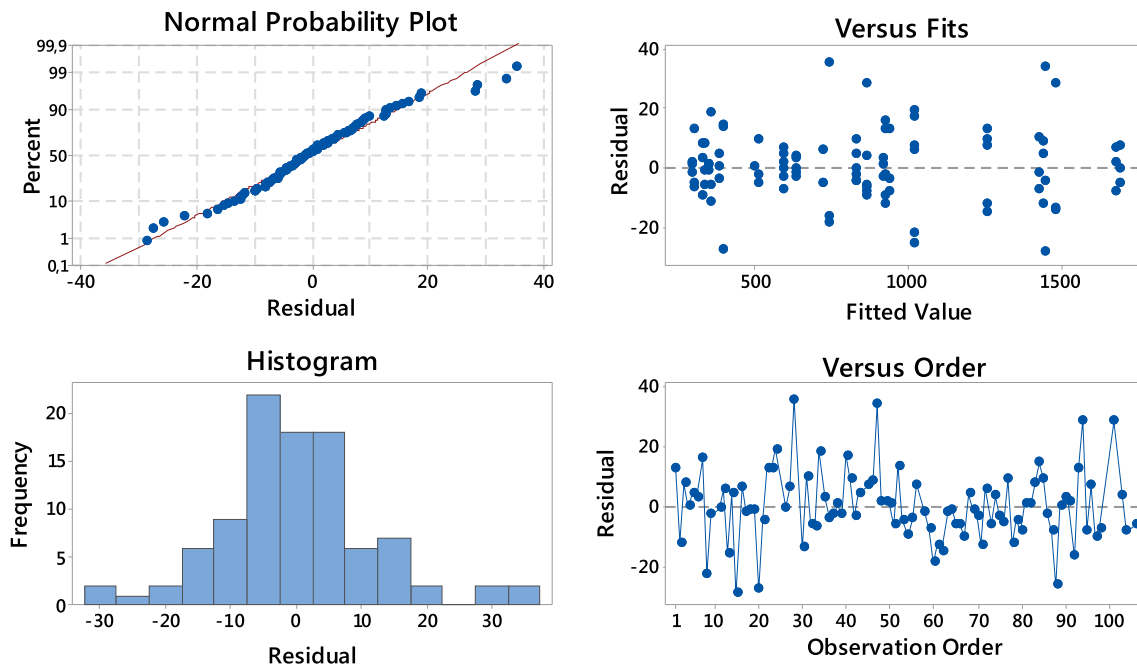
Fig. 10 Residual plots for F_{z_peak} at step 7, $\alpha = 0.01$. p value = 0.031

After that, the regression in uncoded units that represent the phenomenon under investigation, F_{z_peak} in step seven, could be estimated Eq. (2).

$$F_{z\_peak}S7 = -1050 + 117d_t + 20,1\alpha + 2105t + 583\Delta z \\ - 137d_t * t - 1d_t * \Delta z - 38,9\alpha * t - 22,1\alpha \\ * \Delta z - 398t * \Delta z$$

(2)

This equation can be considered statistically accurate and valid, and it describes the statistical relationship between the significant predictors d_t, α, t, and Δz with the answer Y of the mathematical function expressed.

This function can predict the F_{z_peak} response variable for the new observations. In addition, this regression indicates the direction, size, and statistical significance of the relationship between a respective predictor and the dependent variable. It should be noted that $R^2 = 99.92\%$; that is, the model indicates that the four pure predictors and their 5 s order interactions represent 99.92% of the F_{z_peak} S7 forming force in this investigation. So that, it can be written that:

- For each 1 mm increase in tool diameter d_t, the F_{z_peak} is expected to increase by 117 units.
- For each 1 degree increase in the wall angle α, the F_{z_peak} is expected to increase by 20.1 units.
- For each 0.1 mm increase in the sheet thickness t, the F_{z_peak} is expected to increase by 210.5 units.
- For each 0.1 mm increase of step size Δz, the F_{z_peak} is expected to increase by 58.3 units.

4 Conclusion

The vertical step size Δz becomes the most important parameter in this full factorial experiment DoE, 2^5. Thereby, it must be adjusted to the best possible condition in order to minimize the bending effort F_{z_peak} and, so, enable the ISF process to be carried out at the available CNC machining center. The step Δz should be as small as possible within the working ranges and, of course, appropriate to the product geometry, material, and sheet thickness too. Although the sheet thickness t is significant in this experimental design, it is totally dependent on the product design area. On the other hand, the feed rate f could be maximized to produce the part in the shortest time, without losses in terms of overload in the forces. However, it is also necessary to pay attention to any damages that may arise in the part due to the probable vibrations induced to the tool body when at high feeds. Tool diameter d_t is also a significant factor in this investigation in terms of F_{z_peak} force, and there is a slight influence of this parameter on the response variable. Thus, the largest possible diameter could be applied in order to improve the tool stiffness. Meanwhile, a good strategy used to increase the tool stiffness is to manufacture its rod with a diameter larger than the tip that is effectively acting on the forming part, as well as the possibility of applying conjugated tools. The wall angle α is a significant factor in this research and, notoriously, a variable defined by design area. The influence of the wall angle on the forming force is small. But it is possible to exceed the respective limit of the process depending on the

depth at which such complexity must be formed. It could create a risk to the process and even damage the machine, the tool, or the part. In this sense, the wall angle alone does not have a high influence on the generated loads; however, it is quite dependent on the deformation depth desired for the part. Consequently, there is a compromise relationship between the wall angle α and the maximum designed depth for the product that must be considered. Lastly, the ISF process evolution in terms of field application is increasing, necessary and aligned with the technological requirements imposed by the market nowadays.

Compliance with ethical standards

Conflict of interest The authors declare that there is no conflict of interest.

References

1. Ying S (2003) Fundamental studies on the incremental sheet forming of titanium. Bachelor Individual Project, Faculty of Engineering, University of Nottingham, Nottingham
2. Schaeffer L (2004) Conformação Mecânica. Editora Imprensa Livre, p 167
3. Emmens WC, Sebastiani G, van den Boogaard AH (2010) The technology of incremental sheet forming—a brief review of the history. J Mater Process Technol 210:981–997. https://doi.org/10.1016/j.jmatprotec.2010.02.014
4. Schwab K (2016) The fourth industrial revolution, 1st edn. World Economic Forum, Switzerland, p 198
5. Mugendiran V, Gnanavelbabu A, Ramadoss R (2014) Parameter optimization for surface roughness and wall thickness on AA5052 aluminium alloy by incremental forming using response surface methodology. Proc Eng 97:1991–2000. https://doi.org/10.1016/j.proeng.2014.12.442
6. Jeswiet J, Young D (2005) Forming limit diagrams for single-point incremental forming of aluminium sheet. Proc IMechE Part B J Eng Manuf 219:359–364. https://doi.org/10.1243/095440505X32210
7. Mohammad JM, Bijan MD (2012) Analysis of incremental sheet metal forming using the upper-bound approach. Proc IMechE Part B J Eng Manuf 226:1309–1320. https://doi.org/10.1177/0954405412445113
8. Aerens R, Eyckens P, Van Bael A et al (2010) Force prediction for single point incremental forming deduced from experimental and FEM observations. Int J Adv Mfg Technol 46:969–982. https://doi.org/10.1007/s00170-009-2160-2
9. Henrard C, Bouffioux C, Eyckens P et al (2011) Forming forces in single point incremental forming: prediction by finite element simulations, validation and sensitivity. Comput Mech 47:573–590. https://doi.org/10.1007/s00466-010-0563-4
10. Jeswiet J, Micari F, Hirt G et al (2005) Asymmetric single point incremental forming of sheet metal. Ann CIRP 54:88–114
11. Ambrogio G, Filice L, Micari F (2006) A force measuring based strategy for failure prevention in incremental forming. J Mater Process Technol 177:413–416. https://doi.org/10.1016/j.jmatprotec.2006.04.076
12. Duflou J, Tunçkol Y, Szekeres A et al (2007) Experimental study on force measurements for single point incremental forming. J Mater Process Technol 189:65–72. https://doi.org/10.1016/j.jmatprotec.2007.01.005
13. Ingarao G, Ambrogio G, Gagliardi F et al (2012) A sustainability point of view on sheet metal forming operations: material wasting and energy consumption in incremental forming and stamping processes. J Clean Prod 29–30:255–268. https://doi.org/10.1016/j.jclepro.2012.01.012
14. Ambrogio G, Duflou J, Filice L et al (2007) Some considerations on force trends in incremental forming of different materials. AIP Conf Proc 907:193–198
15. Petek A, Kuzman K, Kopac J (2009) Deformations and forces analysis of single point incremental sheet metal forming. Arch Mater Sci Eng 35:107–116
16. Bagudanch I, Garcia-Romeu ML, Centeno G et al (2015) Forming force and temperature effects on single point incremental forming of polyvinylchloride. J Mater Process Technol 219:221–229. https://doi.org/10.1016/j.jmatprotec.2014.12.004
17. Babu SC, Kumar VSS (2012) Experimental studies on incremental forming of stainless steel AISI 304 sheets. Proc IMechE Part B J Eng Manuf 226(7):1224–1229. https://doi.org/10.1177/0954405412441286
18. Li Y, Liu Z, Lu H et al (2014) Efficient force prediction for incremental sheet forming and experimental validation. Int J Adv Mfg Technol 73:571–587. https://doi.org/10.1007/s00170-014-5665-2
19. Ambrogio G, Filice L, Gagliardi F (2012) Formability of light-weight alloys by hot incremental sheet forming. Mater Des 34:501–508. https://doi.org/10.1016/j.matdes.2011.08.024
20. Tiburi F (2007) Aspectos do processo de estampagem incremental. Escola de Engenharia, Universidade Federal do Rio Grande do Sul, BR, Dissertação de Mestrado